Proteomic Study of the Mucin Granulae in an Intestinal Goblet Cell Model

Ana M. Rodríguez-Piñeiro,[†,‡] Sjoerd van der Post,[†] Malin E. V. Johansson,[†] Kristina A. Thomsson,[†] Alexey I. Nesvizhskii,[‡] and Gunnar C. Hansson*[,†]

[†]Department of Medical Biochemistry and Cell Biology, University of Gothenburg, Box 440, 40530 Gothenburg, Sweden
[‡]Department of Pathology, University of Michigan, 1301 Catherine Road, 48109 Ann Arbor, Michigan, United States

Ⓢ *Supporting Information*

ABSTRACT: Goblet cells specialize in producing and secreting mucus with its main component, mucins. An inducible goblet-like cell line was used for the purification of the mucus vesicles stored in these cells by density gradient ultracentrifugation, and their proteome was analyzed by nanoLC-MS and MS/MS. Although the density of these vesicles coincides with others, it was possible to reveal a number of proteins that after immunolocalization on colon tissue and functional analyses were likely to be linked to the MUC2 vesicles. Most of the proteins were associated with the vesicle membrane or their outer surface. The ATP6AP2, previously suggested to be associated with vesicular proton pumps, was colocalized with MUC2 without other V-ATPase proteins and, thus, probably has roles in mucin vesicle function yet to be discovered. FAM62B, known to be a calcium-sensitive protein involved in vesicle fusion, also colocalized with the MUC2 vesicles and is probably involved in unknown ways in the later events of the MUC2 vesicles and their secretion.

KEYWORDS: *mucins, MUC2, secretory vesicles, goblet cell, ultracentrifugation, mass spectrometry, multivariate analysis, ATP6AP2, FAM62B, VAMP-8*
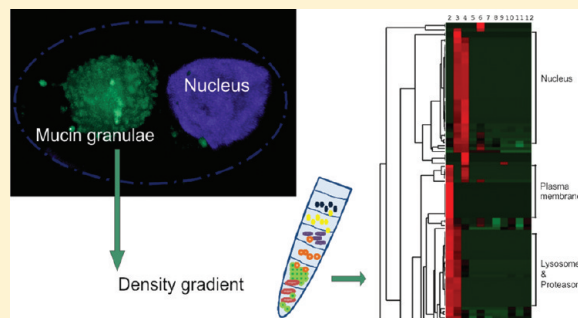
■ INTRODUCTION

Subcellular proteomics is being increasingly applied to resolve the protein content of specific subcellular compartments, find colocalizing proteins, or assign proteins to organelles. These studies usually rely on density gradient ultracentrifugation, where the different organelles separate and can be recovered in independent fractions that can be further analyzed. Proteins from the same organelle should cofractionate and follow the same distribution along one of these gradients. The fractions recovered are normally analyzed by mass spectrometry (MS) techniques, with the identified proteins being generally quantified by protein correlation profiling.[1] Some methods rely on labeling for quantification, as in localization of organelle proteins by isotope tagging (LOPIT),[2] while others are label-free. In the latter, the parameter of choice varies, e.g. the number of ions detected per protein (spectral counts[3,4]), or peptide ion intensities.[5] The most suitable methods to infer conclusions from the huge amount of data generated are usually multivariate tests, which allow grouping of the proteins that follow the same distribution along the gradient. However, a major and inherited problem is that several vesicle types can have similar densities and thus are difficult to separate. This has especially been a problem for vesicles from the regulated secretory pathway, as these vary in density depending on how filled they are.

MUC2 is a gel-forming mucin with more than 5000 amino acids, where the mature and fully glycosylated monomer can reach a mass of 2.5 MDa. MUC2 is dimerized by its C-terminus

in the ER[6] and heavily *O*-glycosylated in the Golgi apparatus, from where it is sorted to the regulated secretory vesicles. Low pH and high calcium concentration trigger N-terminal trimerization[7] at this sorting stage or in the vesicles. When the mucin is released, it has to be unpacked and expanded more than 1000 times to form the mature mucus gel.[8] Packing and release of the MUC2 mucin is a complex but poorly understood process, which generates a well structured and organized inner mucus layer in colon.[8,9] The MUC2 mucin forms the structural skeleton of the inner mucus layer that is firmly attached to the epithelia. This layer acts as a 50−100-μm-thick protective barrier that physically separates the luminal bacteria from the epithelial cells. This inner mucus layer is a major reason for how colon normally can handle the $10^{13}-10^{14}$ bacteria that have their habitat in the outer mucus layer and the colon lumen. A defective inner mucus layer leads to inflammation similar to that observed in ulcerative colitis.[9] To understand this complex process of mucus formation, we need to have deeper insight into how the mucins are stored, how the secretion is mediated, and what molecules other than MUC2 are part of these processes. By using density gradient ultracentrifugation, we have purified vesicles containing the mature form of MUC2 from a differentiating goblet-like cell line.[10] The vesicle proteins were separated by gel electrophoresis

and subjected to proteomic analyses using nanoLC-MS and MS/MS. A number of proteins, previously unknown or already known for being associated with secretory vesicles, were found and further characterized by immunohistochemistry.

■ EXPERIMENTAL PROCEDURES

Cell Culture

The human intestinal goblet-like cell line used was a gift of Clevers[10] and consisted of LS174T cells able to differentiate under the control of a dominant negative form of the TCF4 (dnTCF4), controlled by a Tet-on system. Cells were cultured in Iscove's modified Dulbecco's media (IMDM) with 10% (v/v) fetal bovine serum (FBS), supplemented with sodium pyruvate (110 mg/L), L-arginine (116 mg/L), L-glutamine (290 mg/L), L-asparagine (36 mg/L), folic acid (10 mg/L), and β-mercaptoethanol (3.49 μL/L), at 37 °C in a 5%-CO_2 humidified atmosphere. After reaching 70−80% confluence, they were split by treatment with 0.05% trypsin/0.02% EDTA (w/v) in PBS and subcultured. Once every 4 weeks, cells were selected by adding 500 μg/mL zeocin and 10 μg/mL blasticidin. For differentiation experiments, the MUC2 N-terminal vector pSNMG[7] (4 μg) was transfected into 70%-confluent cells in a 1.9-cm^2 Petri dish 3 h after splitting, using Lipofectamine 2000 (Invitrogen). GFP-expressing clones were selected with 125 μg/mL G418 (Invitrogen) in addition to zeocin and blasticidin. For separation studies, cells were seeded at 5 × 10,000 cells/cm^2 and grown in 23 cm × 23 cm Petri plates. For induction, doxycycline (DOX) was added to the medium at 2 μg/mL for up to 96 h.

Immunostaining of dnTCF4-LS174T Cells

Cells were washed with PBS, fixed in 4% (v/v) paraformaldehyde for 20 min, and permeabilized using 0.1% (v/v) Triton X-100 (Sigma) for 5 min. Unspecific binding was blocked with 20% (v/v) FBS for 20 min. The primary antibody used was anti-MUC2C2[m1] (1/50), a monoclonal antibody against the MUC2 C-terminal peptide CIIKRPDNQHVILKPGDFK. Cy3 goat antimouse Ig G (Invitrogen) was used as secondary antibody (1/3000). UEA1-biotin (1/20; Sigma) was used in combination with streptavidin-FITC (1/100; Dako). The nucleus was stained with DAPI (1/20,000; Sigma). After mounting in ProLong Gold Antifade (Invitrogen), the samples were examined using an LSM 510 confocal microscope with a Plan-Apochromat 63×/1.4 Oil objective (Zeiss). The pictures were analyzed with the Zen 2009 software (Zeiss).

Subcellular Fractionation by Density Ultracentrifugation

All procedures were performed at 4 °C. For fractionation, cells were washed twice with ice-cold PBS, harvested by gently scraping, and centrifugated at 400g for 5 min. Pellets were resuspended in K-Hop buffer (130 mM KCl, 25 mM Tris-HCl, pH 7.5), equilibrated for 15 min, and pelleted again. Precipitates were then resuspended with K-Hop, 0.1% (v/v) DMSO and 2.5× Complete EDTA-free (Roche), and homogenized by passage through syringe needles of decreasing gauge (22G, 25G, 27G). Cell integrity was controlled during homogenization by phase contrast microscopy. Nuclei were removed by centrifugation at 1000g for 5 min.

Organelle separation was achieved through Nycodenz (Axis-Shield) density gradients, which were made with a gradient mixer Hoefer SG 15 (Hoefer) at 750 rpm. For 8−10 mL gradients, a 0.66-mL Nycodenz cushion was laid at the bottom of the gradient, whereas the postnuclear supernatant was carefully added on top. Ultracentrifugation was performed at 100,000g for 90 min in a Beckman Optima L-90K Ultracentrifuge with a

swinging rotor (SW41 Ti, Beckman Coulter). One-milliliter fractions were recovered from top to bottom and diluted 1:1 with K-Hop buffer, and a 5-μL 50%-sucrose (w/v) cushion was added prior to pelleting at 100,000g for 60 min in a Beckman Optimax MAX-E Ultracentrifuge with a fixed-angle rotor (TLA45, Beckman Coulter). Pellets were redissolved in the appropriate buffers for the subsequent techniques. The linearity of the gradients was corroborated by weighting a given volume of each fraction step with a Carlsberg pipet and calculating the linear regression coefficient.

Protein and Mucin Gel Electrophoresis

For general protein separation through monodimensional electrophoresis, fractions were dissolved in reducing sample buffer and separated in 1.5-mm, 4−10% (v/v) polyacrylamide (30% T, 2.6% C) denaturing minigels with a 3% stacking gel, according to Laemmli.[11] SDS-PAGE was performed in a Mini-Protean II apparatus (Bio-Rad) at 90 V. For visualization of protein bands and identification, gels were fixed in 50% (v/v) methanol and 10% (v/v) acetic acid for 1 h, stained with 0.05% (w/v) Coomassie brilliant blue R-250 in the previous solution for 1 h, and destained in 5% (v/v) methanol, 7% (v/v) acetic acid. Precision Plus Protein Standards (Bio-Rad) were used as molecular mass markers.

For mucin detection, samples were prepared in reducing sample buffer and separated in composite agarose-polyacrylamide (Ag-PAGE) gels [1.5 mm; 0.5%−1% (w/v) agarose, 0−6% (v/v) polyacrylamide gradient (40% T, 2.5% C), 0−10% (v/v) glycerol in 0.375 M Tris-HCl pH 8.1] as described before.[12] For visualization, gels were fixed in 50% (v/v) methanol, 1% (v/v) acetic acid for 1 h, equilibrated with 25% (v/v) ethanol and 10% (v/v) acetic acid twice for 15 min, stained with 0.125% (w/v) Alcian blue in the equilibration solution, and destained in 50% (v/v) methanol, 10% (v/v) acetic acid thrice for 10 min.

In-Gel Trypsin Digestion

For identification, each lane from the Coomassie-stained gels was divided into 20 bands, which were cut out and destained with 50% (v/v) ACN and 25 mM ammonium bicarbonate. These samples were dried and digested with 10 μg/mL trypsin (Promega) in 25 mM ammonium bicarbonate at 37 °C overnight. The digestion was stopped, and peptides were eluted with 50% (v/v) ACN and 2% (v/v) TFA. A second extraction was done with 50% (v/v) ACN and 0.2% (v/v) TFA, and extracts were pooled, dried, and redissolved in 18 μL 0.1% (v/v) formic acid.

Protein Identification by Mass Spectrometry and Relative Quantification

Samples were analyzed by nanoflow reverse-phase LC-ESI MS/MS (LTQ Orbitrap XL, Thermo Scientific) as previously described.[13] Briefly, 2 μL of the digest were injected using a HTC-PAL autosampler (CTC Analytics AG) connected to an Agilent 1100 capillary pump (Agilent Technologies); peptides were trapped on a precolumn (4 cm long × 100 μm inner diameter) set up in a valve-switching configuration. After 5 min of loading in 0.2% (v/v) formic acid (buffer A), the peptides were eluted over the analytical column (20 cm long × 50 μm inner diameter) with a linear gradient over 40 min [5−50% buffer B, 100% (v/v) ACN] at a split flow rate of ∼100 nL/min. The columns were packed with ReproSil-Pur C18-AQ 3 μm resin (Dr. Maisch, GmbH). MS data were acquired in a data-dependent mode automatically switching between MS and MS/MS acquisition. Full MS scans were obtained in the Orbitrap at 400−2000 m/z, 2 microscans, maximum ion injection time

500 ms, and a target value of 500,000, using the lock mass feature for internal calibration (m/z 445.1200). Resolution was set to 60,000 at m/z 400. MS/MS was performed in the linear ion-trap on the six most abundant multiply charged ions for each scan (1 microscan, isolation window of 3 amu, maximum 200 ms ion injection, and a target value of 10,000), using CID fragmentation at 30% normalized collision energy. After fragmentation, peptides were excluded for 3 s for further acquisition. Spectral data were processed into peak lists using the Quant module in MaxQuant (v. 1.0.12.31)[14] without pair detection, and they were searched using the MASCOT search engine (version 2.2, MatrixScience). The searches were performed against the international protein index (IPI) database (v. 3.52, 73,667 protein sequences) appended with a decoy database and common contaminants. Search parameters were set as follows: (i) enzyme trypsin, maximum 1 missed cleavage allowed; (ii) 7 ppm precursor mass tolerance and 0.5 Da for fragment ions; (iii) charge state +1; (iv) fixed modification propionamide (C), and variable modifications oxidation (M) and acetylation (protein N-term). Relative quantification was performed on the basis of the combined ion chromatogram over the elution profile for each identified peptide, extracted into a three-dimensional peak. Identifications and quantifications were combined using the identify module in MaxQuant, applying a false discovery rate (FDR) for both peptide and protein identification at 0.01%; protein identification was based on a minimum of 1 unique peptide, and proteins were grouped when based on the same set of peptides. All identified proteins and their descriptions (i.e., grouped entries, unique peptides, and sequence coverage) can be found in Table S1 of the Supporting Information. Only protein identifications based on a minimum of two peptides were selected for further colocalization studies. Peptide three-dimensional peak intensities were assigned to proteins, and both unique and nonunique peptides were used for quantification. Nonunique peptides were strictly used for the quantification of the protein with the most assigned peptides.[14] Total protein quantity was calculated for each individual protein by summing the total intensity per gel lane. The protein intensity over the complete gel was used to determine the protein distribution over all lanes when identified in at least two replicates. Protein distribution was evaluated using hierarchical cluster analysis: total protein intensities were normalized to 1, and Cluster (v. 3.0[15]) was employed for the analysis, using "Euclidean distance" as similarity metric combined with average linkage clustering.

Selection of Organelle Markers and Statistical Methods

The proteins employed as organelle markers were extracted from previously published studies[3,5,16] and from the information contained in Swiss-Prot (UniProt KB[17]). Protein gene ontology (GO) cellular component enrichment in the different fractions was performed using DAVID (Database for Annotation, Visualization and Integrated Discovery).[18] The enrichment analysis was based on the annotation of all proteins identified compared to that of the individual fractions. GO cellular component data were clustered when the GO term was enriched in at least one fraction ($p < 0.05$), fractions without values were given a standard p-value of 1[19] and log-transformed, and finally the data were transformed into z-scores. The enrichment analysis-based organelle distribution was compared with the protein profile of the known organelle markers for validation. For principal component analysis (PCA), the relative quantity of each protein in each lane was imported into the SPSS software package (v. 17). Only the proteins found in the three replicates were considered, in order to get comparable principal components (PCs), avoiding the problem of inferring

null values. PCs with *eigenvalue* > 1 were retained as variables. As the PCs are orthogonal by definition, those with higher information for the proteins selected as organelle markers were plotted, in order to evaluate if the distribution per lane in the density gradient was consistent with organelle integrity and with results from published density separations. Bivariate Pearson correlations between replicates were calculated on the basis of the first PC obtained for each data set. Correlations were significant at the 0.01 level (99% confidence).

Immunolocalization in Colon Tissues

Biopsies were obtained from normal controls referred to colonoscopy at Sahlgrenska University Hospital (Gothenburg, Sweden). All patients had a normal mucosa upon visual examination by the endoscopist. Informed consent from these patients was obtained in writing. The study was approved by the Human Research Ethical Committee of the Medical Faculty, University of Gothenburg, Gothenburg, Sweden. Tissues were fixed in Carnoy solution (60% ethanol, 30% chloroform, and 10% glacial acetic acid) and sectioned as described before.[20] Carbachol (CCH)-stimulated specimens and the corresponding controls were a generous gift from J. K. Gustafsson. The anti-MUC2C2[m1] antibody was used as a 1/20 dilution; other antibodies were raised in rabbit (Atlas Antibodies) and used as follows: 1/100 anti-ATP6AP2, 1/250 anti-FAM62B, 1/250 anti-PLXNA1, 1/500 anti-RAB3A, 1/200 anti-SDF4, 1/100 anti-TMED2, 1/100 anti-VAMP-7, 1/500 anti-VAMP-8. As secondary antibodies we employed 1/2000 Alexa Fluor 488 goat antimouse Ig G (H+L) or Alexa Fluor 555 goat antirabbit Ig G (H+L) (Invitrogen). DNA was stained with 1/20,000 DAPI (Sigma). Samples were mounted with ProLong Gold Antifade (Invitrogen). Fluorescence images were obtained on a LSM 700 Axio Examiner.Z1 laser scanning confocal microscope, with a Plan-Apochomat 40×/1.3 Oil DIC objective and analyzed with the Zen 2009 software (Zeiss).

■ RESULTS AND DISCUSSION

The MUC2 Mucin Producing LS174T Cell Line

To isolate the regulated vesicles storing the MUC2 mucin, we used the goblet-like dnTCF4-LS174T cell line developed by Clevers' group.[10] This cell line permanently expresses a dominant negative form of the TCF4 transcription factor under the control of tetracycline. This allows the expansion of the cell number, until the addition of tetracycline (or its analog doxycycline) causes the cells to stop dividing and to differentiate into cells with goblet cell morphology. It was previously shown that these cells accumulate the MUC2 mucin;[10] the localization of the mucin to vesicles that gather in a typical goblet cell theca is shown in Figure 1A by staining with the fucose-binding UEA1 lectin. The information for localizing the MUC2 mucin to the regulated secretory pathway is found in the N-terminal 1397 amino acids, as transfection of dnTCF4-LS174T cells with a plasmid encoding these amino acids fused with EGFP localized the recombinant protein to the mucin vesicles. When these cells were induced to differentiate for 96 h, the fluorescent MUC2 N-terminus accumulated in vesicles that formed a typical goblet cell theca (Figure 1B). These vesicles also carried the endogenous full-length MUC2 mucin (Figure 1C).

Purification of the MUC2 Mucin Vesicles by Density Gradient Ultracentrifugation

To reveal the proteins associated with the goblet cell granulae, we performed a subcellular fractionation of these cells using Nycodenz density gradients and ultracentrifugation. The linearity
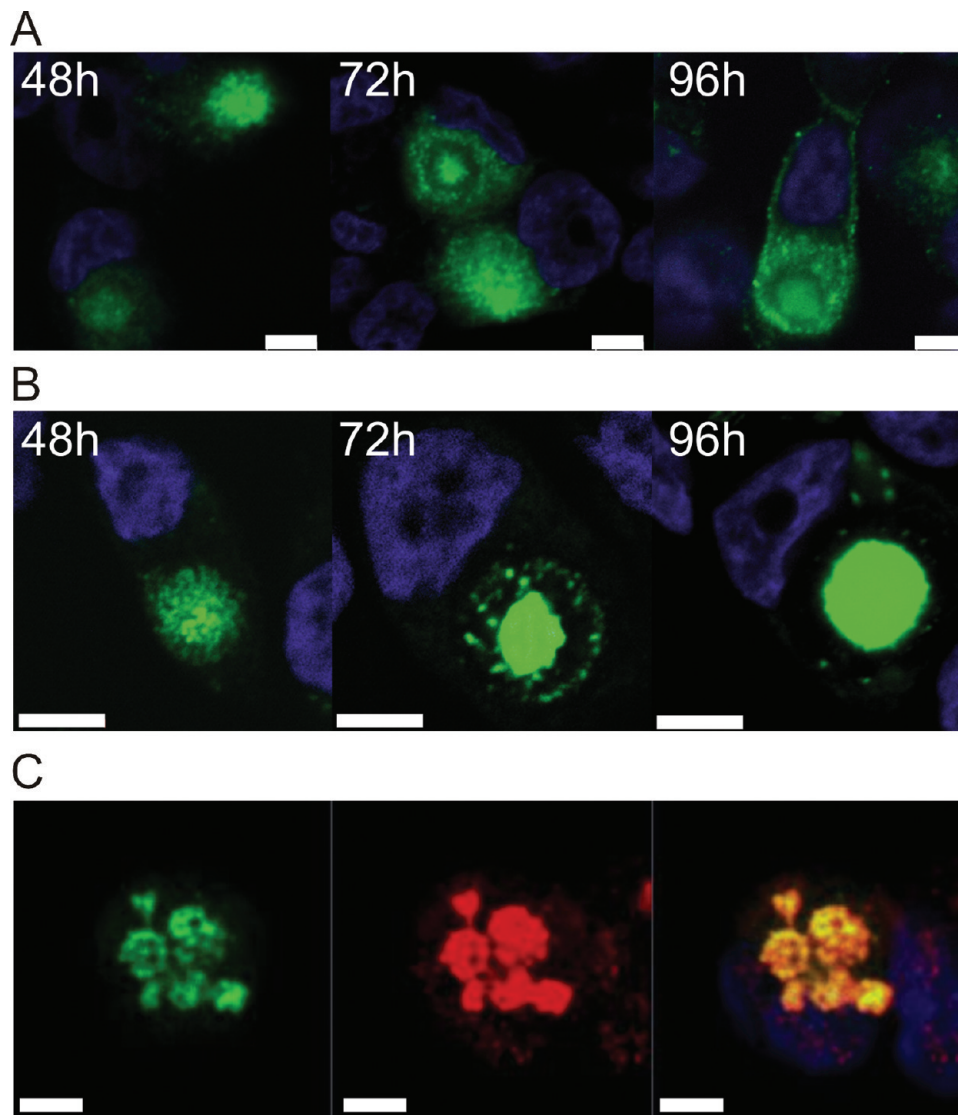
Figure 1. The dnTCF4-LS174T cells form typical goblet cell mucin granulae and theca after differentiation. The dnTCF4-LS174T cells were induced 48−96 h with doxycycline to express the dominant negative transcription factor TCF4. (A) Staining of fucose by the *Ulex europaeus* lectin 1 (UEA1). (B and C) The dnTCF4-LS174T cells were transfected with a plasmid encoding the N-terminal 1397 amino acids of the MUC2 mucin fused with EGFP. (B) Fluorescent vesicles accumulate into a theca by differentiation. (C) The fluorescent vesicles containing MUC2-N-EGFP (green) were also stained by the anti-MUC2C2[m1] reacting with the C-terminus and detecting the endogenously expressed MUC2 (red). Nuclei labeled with DAPI (blue). Bar size 5 μm.

of the gradients was corroborated for different ranges, showing an average coefficient of correlation with the bisectrix of 0.92 (standard deviation of 0.049). The fractions collected were analyzed by PAGE and stained with Coomassie to visualize proteins, and with Alcian blue to specifically detect the negatively charged mucins. A standard 2−25% Nycodenz gradient with collection of 11 fractions showed a good separation of the whole protein content (Figure S1A of the Supporting Information). Detection of ER and Golgi markers by Western blot showed a wide separation of these organelles, which extended over three or four fractions (Figure S1B). The band with the reduced highly glycosylated MUC2 mucin monomer was found with high molecular mass, mostly in fractions 3−6, on composite agarose-PAGE (Ag-PAGE) after Alcian blue staining (Figure S1C and 1D, marked MUC2). Other forms of less glycosylated MUC2 were found in most fractions, especially in those corresponding to the ER (as discussed in the next section). This is consistent with previous observations that vesicles of the secretory pathway first

decrease in density and that vesicles sorted to the regulated secretory pathway then increase in density and thus move "back" into less mature and denser vesicles.[21] Therefore, the goblet cell mucin storage granulae appeared at several densities and were mixed with other granulae, for example from the Golgi stack.

To obtain purer mucin vesicles, we tested a number of other density gradients. Besides, we tested combinations of two sequential gradients, but the overall quality of the separation did not improve. The best focusing of the mature mucin vesicles was obtained when the ultracentrifugation was done in a single gradient of 10−48% Nycodenz (Figure 2). This gradient was used for the subsequent studies. The results presented are based on three replicates to account both for biological and technical variability. This means that the cells were cultured in three independent plates, induced to differentiate for 96 h, and processed separately. Two of the replicates were processed in parallel, while the third was processed at a different occasion.
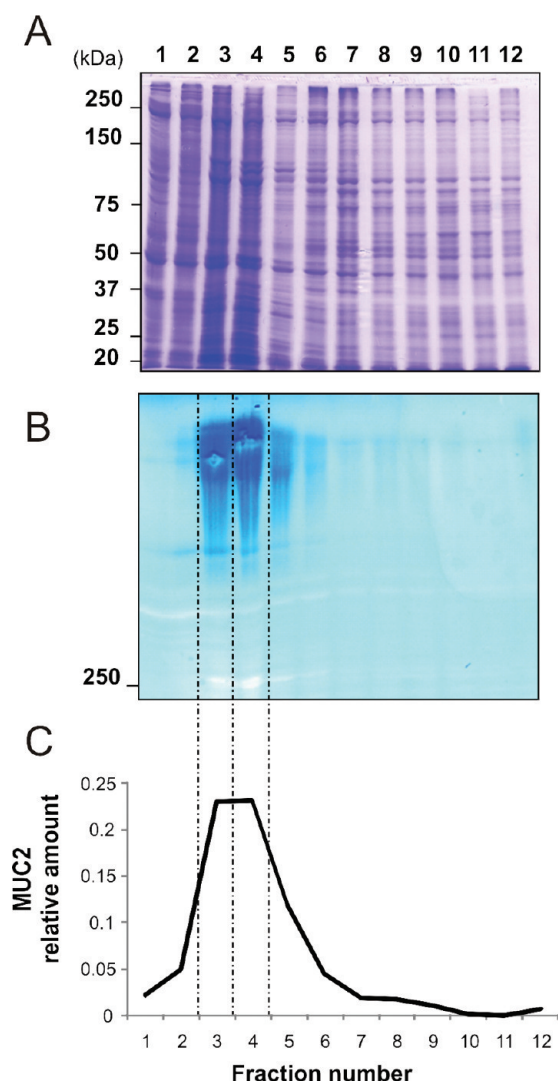
Figure 2. Separation and analysis of 12 fractions obtained from 96-h-induced dnTCF4-LS174T cells on a 10−48% Nycodenz gradient with a 50% bottom sucrose cushion. (A) Coomassie-stained PAGE (4%−10%) showing the protein profile in the fractions. (B) The obtained fractions were analyzed by Ag-PAGE and stained with Alcian blue to visualize the distribution of the highly glycosylated mature mucins. (C) Relative amount of mature MUC2 as calculated from the gel in part B.

Proteomic Analysis

The obtained fractions were separated and trypsin-digested before nanoLC-MS/MS using an LTQ-Orbitrap mass spectrometer. We recovered 12 fractions from each gradient but did not include the first fraction in our studies, as the soluble proteins collected there would bias our cluster analyses. Each of these fractions was analyzed, and using the inclusion criteria of at least one unique peptide per protein, and a maximum peptide false discovery rate of 0.01%, the protein composition was determined, as shown in Table S1 of the Supporting Information for the three replicates. We then compared the fractions between the replicates and the total number of proteins in each replica. We identified an average of 2,616 ± 238 proteins per sample, with 1972 of them shared between the three replicates (Figure S2). Next, we analyzed the distribution of proteins among the fractions in each replica, and for this we discarded the proteins that appeared only in one of the replicates. A total of 2570 proteins were finally considered. The identified proteins and

the corresponding peptide information after MS identification can be found in Table S1.

An obstacle in the localization of the MUC2 vesicles in the density gradient is that MUC2 is also present in the ER, the Golgi, and different types of vesicles trafficking through the secretory pathway. The MUC2 mucin is highly glycosylated, polymerized, and densely packed when stored in the mucin vesicles. Without reduction of its numerous disulfide bonds, the mucin is insoluble, but even after reduction and trypsin digestion, the MUC2 mucin yields few peptides due to the large number of glycans.[6,22] Many of the obtained peptides are modified with glycan moieties, making typical database identification impossible, generating only a few hits for such a large protein. As the MUC2 precursor forms are less glycosylated and polymerized, there was an overrepresentation of hits for the MUC2 forms found in the ER and Golgi. Thus, we could not use the MUC2 peptides for tracking the secretory vesicles. Instead, we took advantage of the large size and stainability of the mature, heavily glycosylated MUC2 with Alcian blue on Ag-PAGE gels. Thus, the relative quantity of MUC2 in each fraction was used to track the vesicle distribution, as exemplified in Figure 2C for one of the replicates. To ensure that the results were not biased, equal sample aliquots were loaded onto the gels used to cut bands for MS analysis and the Ag-PAGE gels used to quantify the mucin amount. To verify that the Alcian blue stain on the Ag-PAGE gels was indeed MUC2, several bands per lane were digested with trypsin and analyzed by mass spectrometry. Table S2 of the Supporting Information is a summary of the MUC2 peptides identified.

Different quantitative proteomics methods can be used in high-resolution mass spectrometry. Here we used a label-free approach where extracted ion chromatograms of the identified peptides over their chromatographic peaks were used to relate protein abundance in the different density gradient fractions. Summed protein ion-current profiles from subsequent gradient fractions were plotted to determine the distribution of each individual protein and to classify them by organelle using correlation profiling. We analyzed the organelle separation on the basis of the protein abundance distributions by several independent methods. First, we employed principal component analysis (PCA) to reduce the amount of information contained in the results to a few variables that could be examined (principal components, PCs). As the PCs summarize the variability in a data set, we hypothesized that if the density gradient separations were reproducible, the information should be similarly divided into the PCs, and the correlations between the PCs should be significant and high. To corroborate this, we applied the Pearson test to the first PC (PC1) calculated for each of the almost 2000 proteins identified in all three replicates. The PC1 accounted for about 30% of the variance in all the replicates. As shown in Figure 3A, the Spearman correlation coefficients (r) were as follows: 0.881 between replicates 1 and 2 (run in different day); 0.911 between replicates 1 and 3 (run in different day); and 0.931 between replicates 2 and 3 (parallel experiments). All the r values were significant at the 99% confidence level ($p > 0.01$). Thus, these values indicate a high correlation between the distribution of the relative quantity of the 1972 proteins identified along all three replicate density gradients, confirming the reproducibility of both biological and technical replicates. The coefficients obtained are in accordance with others previously reported after multivariate analyses; the most comparable study we found was the analysis of a lymphocyte cell line labeled with iTRAQ, where a correlation coefficient of 0.85 between the two replicates was observed for 1090 proteins.[16] Since replicate 3 (R3) showed the highest correlation with the other two replicates, we chose this as the most
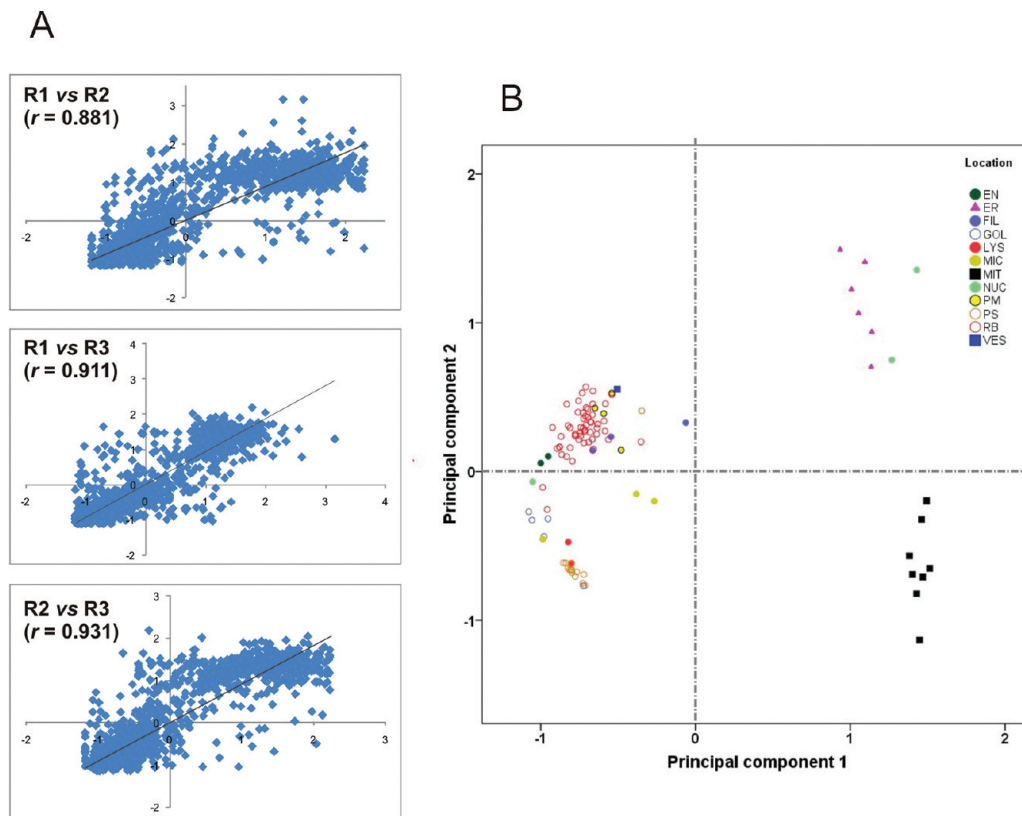
Figure 3. Bivariate correlations between the three biological replicates on the basis of their first principal component (PC1) and plot of organelle markers. (A) Correlation between the three replicates (R1, R2, R3). The replica R3 was considered the most representative and, hence, was used to present the results. (B) Plot of the markers employed in the study separated by their first two principal components. Notice the clear division between "light" (PC1 < 0) and "heavy" (PC1 > 0) organelles. EN, endosomes; ER, endoplasmic reticulum; FIL, filaments; GOL, Golgi apparatus; LYS, lysosomes; MIC, microtubules; MIT, mitochondria; NUC, nucleus; PM, plasma membrane; PS, proteasome; RB, ribosomes; VES, vesicles.

representative one. Therefore, figures in this article refer to this replicate, although all calculations and data processing were done for the three data sets and results averaged/pooled.

Apart from assessing the reproducibility of the method, PCA allowed us to corroborate the separation of different organelles, simply by plotting the coordinates given to certain proteins known as markers for that cellular location. We obtained a very clear separation between organelles considered as heavy, such as mitochondria and ER, and lighter ones, such as the Golgi (Figure 3B).

A more generic method to evaluate the organelle distribution is enrichment analysis based on protein functional annotation, retrieved from databases such as GO and KEGG.[19] In Figure 4 we plotted the proteins identified in the different fractions (contained in Table S1 of the Supporting Information), after cluster analysis on the basis of their GO cellular component terms. Sections along the cluster highlight organelle locations. The GO cellular component analysis was consistent with the subcellular localization of known protein markers, as shown by plotting their abundance along the gradient fractions. The markers used for this analysis are highlighted in Table S1.

Proteins Clustered with the Mature MUC2 Mucin

To find the proteins that colocalize with the mature MUC2 in the mucin granulae, we selected 205 proteins that peaked in either fraction 3 or 4 correlating with the MUC2 staining (Figure 2C), marked in Table S1 of the Supporting Information. Each of these proteins was individually analyzed by four of the authors in an independent manner, studying its function and potential

relation to vesicle trafficking, as for example SNARE-related, RAS, vesicle-associated, potentially secreted, and membrane-spanning proteins. On the basis of published literature, we short-listed proteins that could be related to MUC2 mucin storage and secretion, and when available we obtained antibodies for immunofluorescent detection of these proteins. Thus, we examined the localization of the proteins ATP6AP2, FAM62B, PLXNA1, RAB3A, SDF4, TMED2, VAMP-7, and VAMP-8, in relation to MUC2 in human colon biopsies. The localization of these proteins in human sigmoid colon tissue sections is shown in Figures 5 and 6.

The first three proteins discussed here are shown in red in Figure 5A. Plexin-A1, PLXNA1 (accession number Q9UIW2), is a receptor for class II and class IV semaphorins involved in cell adhesion, migration, and axon guidance through its effects on cytoskeleton remodeling. Interestingly, it was recently shown that it participates in promoting actomyosin contraction in the rear side of dendritic cells, through its interaction with semaphorin Sema3A.[23] This protein was found in goblet cells but largely surrounding the nuclei and with no obvious localization to the mucus granulae. However, a role for PLXNA1 could be speculated in the migration of the mucin granules to the apical side of the goblet cells. SDF4 (Q9BRK5), or Cab45, is a 45 kDa calcium-binding protein that resides in the Golgi and may regulate calcium-dependent activities. A splice variant called Cab45b has been identified in pancreatic acini as an interaction partner for Munc18b and syntaxins 2 and 3, and therefore may be involved in the exocytosis of zymogens by pancreatic acini.[24] In our case, the staining around the nucleus seems to be related to the Golgi
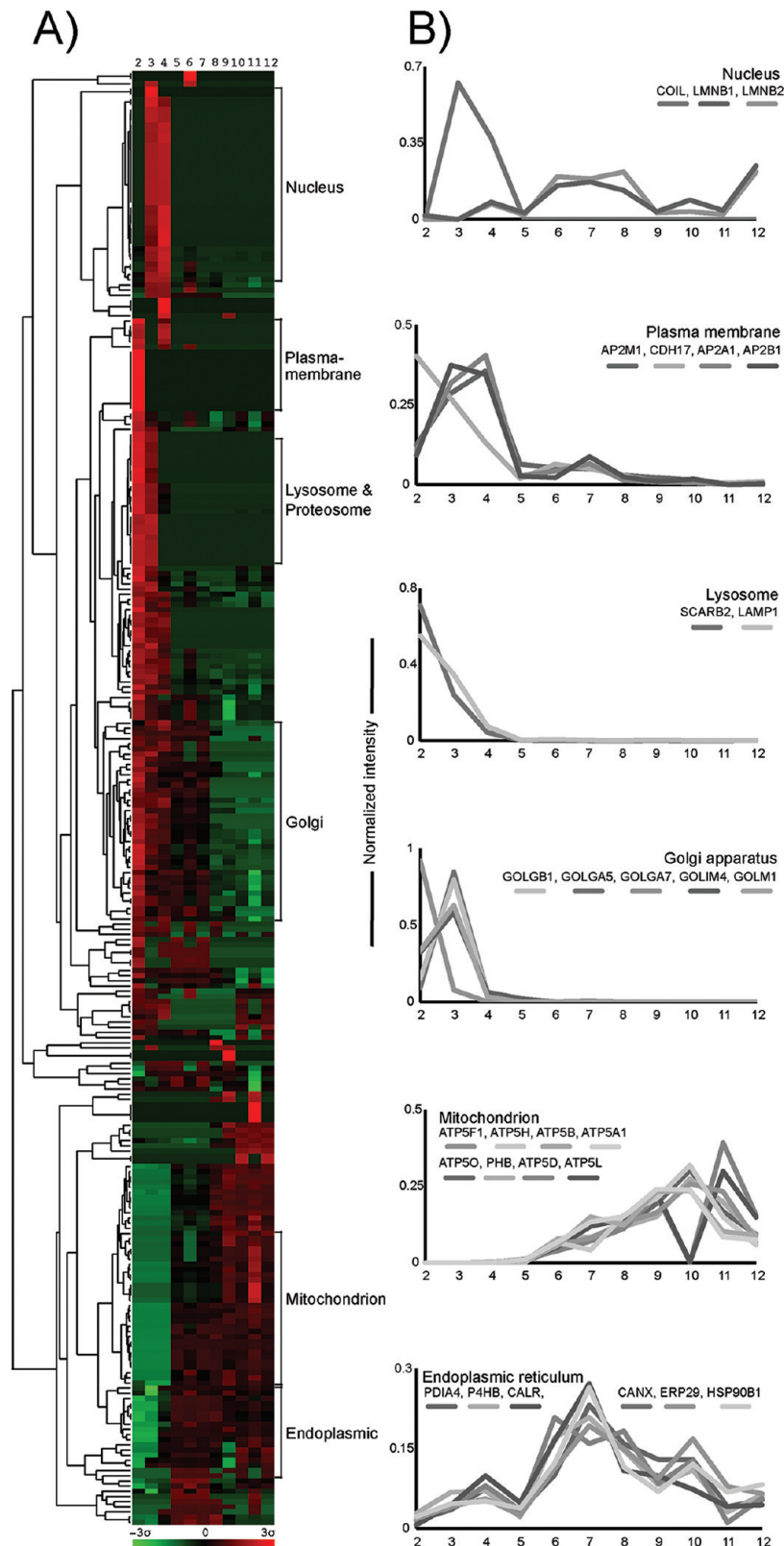
Figure 4. Quality of the organelle separation assessed by hierarchically clustering enriched GO terms for the cellular component in the individual fractions, complemented with the distribution of known organelle markers. (A) The central plot shows the enrichment of organelles for the different fractions in the replica R3, based on GO annotation. (B) Plots of the relative protein abundance of known organelle markers over the fractions analyzed.

calcium-binding function first proposed for the full-length protein. TMED2 (Q15363, transmembrane emp24 domain-containing protein 2), or p24A, has been recently identified in protein-cargo recognition and vesicle budding during vesicular transport between the ER and the Golgi apparatus.[25] The supranuclear staining observed in our study is well in line with a role in the formation of mucin vesicles or earlier events in the secretory pathway.
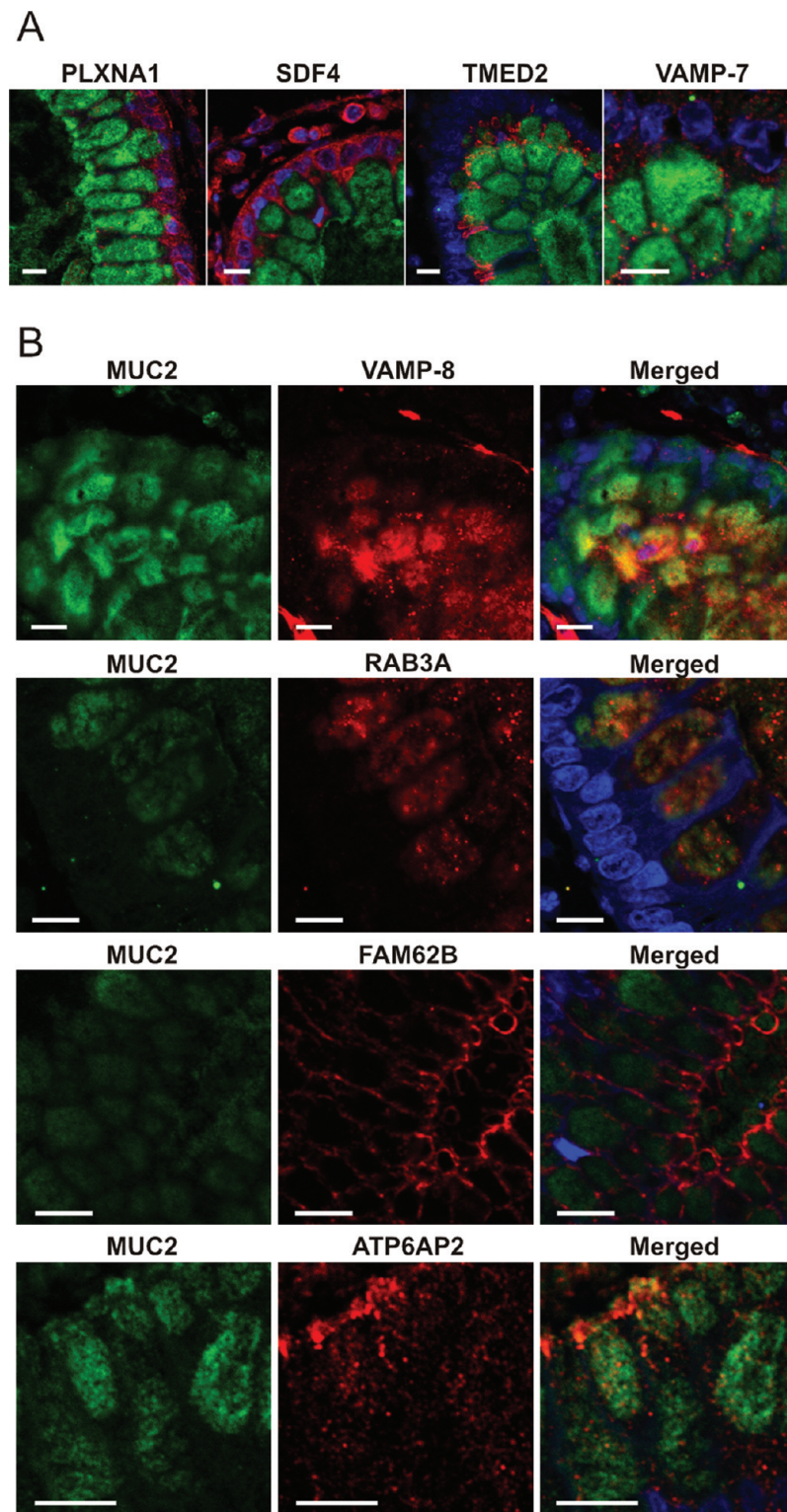
Figure 5. Localization of proteins identified and suggested to be associated with the MUC2 mucin vesicles in human sigmoid colon as studied by confocal microscopy: (A) Co-staining MUC2 (anti-MUC2C2^m1, green) and PLXNA1, SDF4, TMED2, and VAMP-7 (all red) did not show major colocalization; (B) Immunostaining of MUC2 (anti-MUC2C2^m1, green) and VAMP-8, RAB3A, FAM62B, and ATP6AP2 (all red) showed FAM62B lining the apical side of the goblet cells, and the other proteins with different degrees of colocalization with MUC2. Nuclei labeled with DAPI (blue). Bar size: 10 μm.

VAMP-7 and VAMP-8 (P51809, Q9BV40) are the vesicle-associated membrane proteins 7 and 8, respectively. They belong to the synaptobrevin family and are membrane-associated proteins related to the secretion of vesicles. VAMP-7 and VAMP-8 have been localized in eosinophil and neutrophil granulae,[26] and VAMP-8 is proposed to function as an R-SNARE for the secretion of mucins in Calu-3 cells.[27] Staining of the human colon sections with anti-VAMP-7 antibodies revealed dotted staining around the MUC2 mucin vesicles and especially at the apical side of these (Figure 5A). For VAMP-8, a diffuse costaining with MUC2 was observed at the apical side of the theca inside the goblet cells but also outside in the crypt lumen (Figure 5B). In the
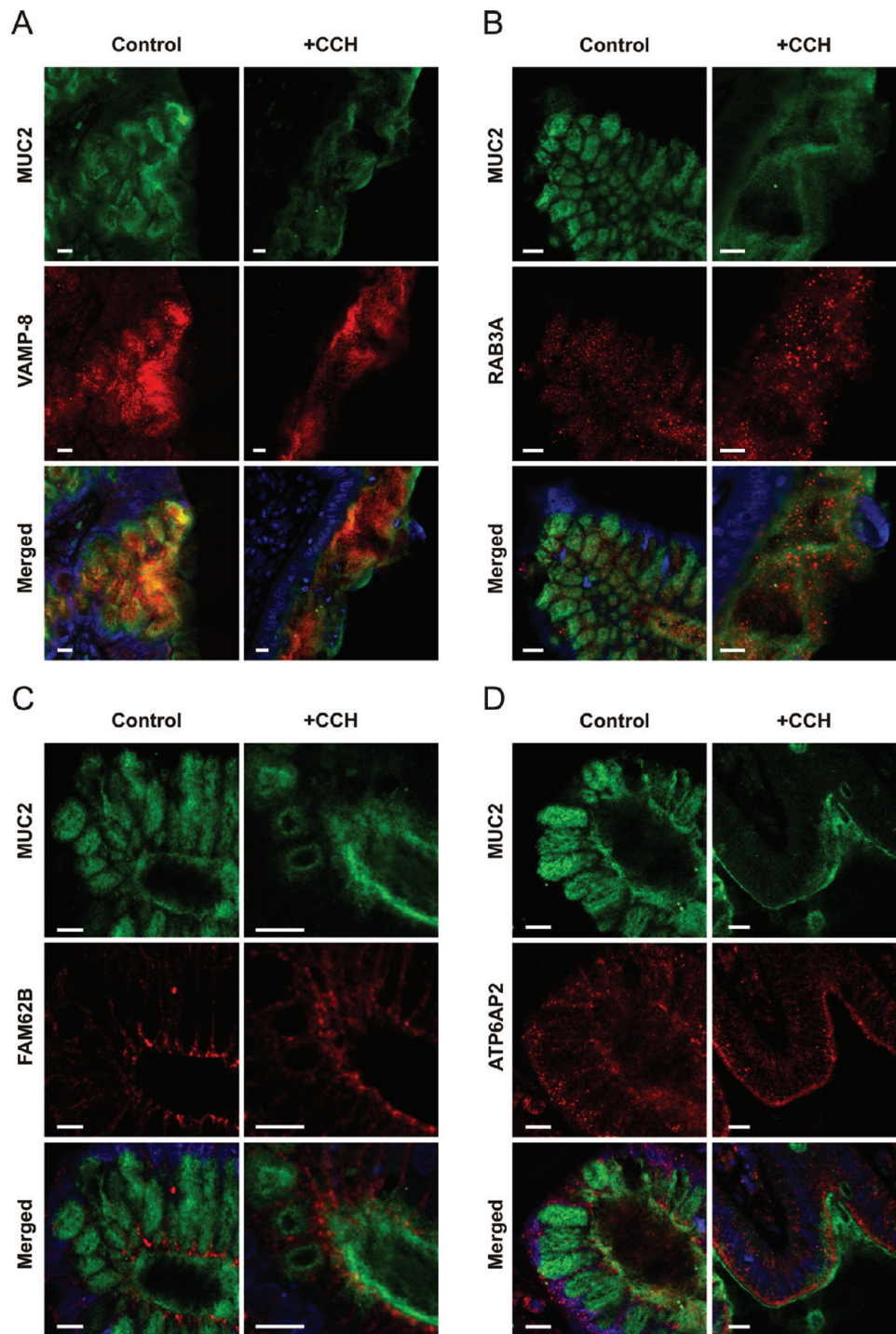
Figure 6. Stimulation of mucin secretion with carbachol resulted in retention of some proteins and secretion of others together with MUC2 as shown by confocal microscopy on human sigmoid colon. Co-staining of MUC2 (anti-MUC2C2^{m1}, green) and VAMP-8 (A, in red) or RAB3A (B, in red) showed a surprising secretion/shedding of these proteins upon carbachol (CCH)-driven stimulation of MUC2 secretion. On the contrary, FAM62B (C, in red) and ATP6AP2 (D, in red) did not show a change in protein location upon stimulation. Nuclei labeled with DAPI (blue). Bar size: 10 μm.

dnTCF4-LS174T cells, VAMP-8 showed a pattern similar to the one in tissues with VAMP-8 surrounding MUC2 vesicles. Our results suggest that at least VAMP-8 is involved in MUC2 vesicle release. A recent study on the Weibel−Palade bodies (WPB) found in endothelial cells proposed a multigranular exocytosis for the von Willebrand factor (VWF). This protein has striking similarities to MUC2 in the arrangement of its N- and C-terminal domains and its mechanism of sorting to regulated vesicles. In the VWF case, it seems that multiple WPB coalesce into a larger structure, named a "secretory pod", before fusing with the cell membrane. It was hypothesized the VWF can only unfurl in these structures after fusing with small nanovesicles (30−40 nm) that might affect the pH to trigger the conformational changes needed.[28] Our observation that VAMP-8 partly colocalizes with the MUC2 vesicles could well correspond to such a mechanism of exocytosis. It shall be noted that VAMP-8 is also found in the material secreted out in the lumen together with MUC2 after carbachol stimulation (Figure 6A).

RAB3A (P20336; Ras-related protein Rab-3A) is involved in the regulation of exocytosis by a late step in vesicle fusion, which is related to vesicle priming.[29] In mouse synapses, for example, RAB3A maintains the pool of fusion-competent vesicles tightly coupled to Ca^{2+} channels.[30] In neuronal vesicles, RAB3A directly binds myosin-Va, and the complex is involved in the transport of these granulae.[31] The protein is partly colocalized with MUC2 as it stains vesicles in the apical part of the colon goblet cells (Figure 5B) and it is found secreted/shed out to the lumen in response to a stimulation of mucin secretion (Figure 6B).

Mucins can be secreted by normal single-vesicle fusion with the membrane or by compound exocytosis. The later type occurs after stimulation with secretagogues, and in this case, the vesicles are fused with each other while still inside the cell, and the large vesicle complexes are then secreted.[32] Electron microscopy pictures suggest that the whole apical part of the cell is lost and, thus, this is not a normal plasma membrane fusion. The mechanisms of this type of secretion are not understood, at least at the molecular level. As RAB3A and VAMP-8, both cytosolic components, were found in the secreted material, it is obvious that, at least under carbachol stimulation, also nonfused intact vesicles can be released from goblet cells.

FAM62B (O75787) is better known as extended-synapto-tagmin 2 (E-Syt2). It contains C(2) domains capable of Ca^{2+}-dependent phospholipid binding and is targeted to the plasma membrane.[33] Recently it was found to be involved in rapid endocytosis of activated FGF receptors in *Xenopus*, and therefore, it has been proposed as an endocytic adaptor in the clathrin-mediated pathway.[34] Staining of FAM62B showed that it surrounded the MUC2 vesicles at the apical surface of the goblet cells (Figure 5B). The distribution of FAM62B is bimodal, with a peak in fraction 4 with mature MUC2, and another one in fraction 7, which is largely ER. Interestingly, the ATP6AP2 protein discussed below shows a similar distribution, while none of them display any major immunostaining over the ER. This may suggest these two proteins are localized together in another vesicle type with a density similar to that of ER. Also to notice, neither of them is secreted/shed to the lumen when mucin secretion is stimulated by carbachol (Figure 6C and D). Altogether, our data and the recent literature make it tempting to speculate a role for FAM62B in the regulation of the signal for mucin vesicle exocytosis.

ATP6AP2 (O75787), ATPase H⁺-transporting lysosomal accessory protein 2 or renin receptor, has been suggested to be a component of the vacuolar proton pump. This is a trans-membrane protein, but in contrast to the V-ATPase components, it has only a short cytoplasmic tail and instead a large vacuolar part. Its function is not known, and it has been recently suggested this protein can sense the levels of acidity in intra-cellular compartments and by this regulate the V-ATPase activity.[35] This should be in line with the V-ATPase that is known to be responsible for the acidification of secretory granules.[36] However, the staining as revealed in Figure 5B is apical to the majority of the MUC2 vesicles, and not over the Golgi and TGN, where staining would have been also expected while suffering progressive acidification.[37] Interestingly, we also found the accessory protein 1 (ATP6AP1) in our set of protein candidates, but none of the "true" components of the V-ATPase. This suggests that these proteins have a role unrelated to the proton pump function of the V-ATPase.

As suggested before and from Figure 1, the MUC2 mucin is the key cargo in the mucin granules. Proteins sorted to the regulated secretory pathway normally show low pH and high calcium-triggered self-aggregation, as is also suggested for the mucins and here shown in Figure 1B by the accumulation of the MUC2 N-termini. This is also supported by the observation that mice defective in the expression of intestinal MUC2 have goblet cells that do not present any of the typical mucin granules.[9,38] This interpretation is further corroborated by our observations that MUC2 appears to be the main, or maybe only, luminal component, as we did not find any other soluble, secreted proteins colocalizing with MUC2 in these cells.

The purification of granulae containing mucins is particularly difficult, as the rupture of only a small proportion of such vesicles would ruin the experiment, since mucins have an intrinsic ability to expand 1000-fold and trap other proteins and vesicles. The approach used here, and especially the use of Nycodenz as density gradient media, circumvented this problem.

The degree of cross-contamination in subcellular proteomic studies is always an issue. For instance, in a specific study of the secretory pathway, quantitative proteomics of highly enriched samples containing mostly Golgi, microsomes, and vesicles showed that approximately 20% of the proteins belonged to other organelles than the ones studied in each fraction.[3] Recently, Andreyev et al.[39] discussed nuclear contamination of postnuclear fractions (which we also experienced in our study), which can be due to cross-contamination, to the proteins being normally pre-sent in multiple organelles, or to other factors. For example, in mouse liver it has been estimated that 39% of the proteins have more than one location.[5] In our study cross-contamination was expected with cytoskeletal components, as these form a meshwork closely associated with the granules and their migration in the cell.[40,41] However, as discussed above for FAM62B and ATP6AP2 in relation to the ER, there could also be several types of vesicles with different origins but the same density, especially vesicles from the regulated secretory pathway, as these become increasingly denser and as a result "move back" toward the dense ER vesicles. These obstacles make the purification and characterization of these type of granulae especially difficult.

■ CONCLUSIONS

Separation and analysis of vesicles belonging to the regulated secretory pathway in goblet cells is a difficult task, as these vesicles have a high density and the mucins they contain have an intrinsic property to trap everything if ruptured. The goblet cell vesicles contained, as expected, the MUC2 mucin, but a few other proteins could be identified by multivariate analyses and immunohistochemical studies to have the potential of being involved in mucin vesicle secretion. VAMP-8 and RAB3A have been shown to be part of this process before, whereas FAM62B and ATP6AP2 are novel potential actors in this system. How-ever, further insights into the function of these proteins demand more functional studies.

■ ASSOCIATED CONTENT

Ⓢ Supporting Information

Supplementary Figures S1 and S2 and Supplementary Tables S1 and S2. This material is available free of charge via the Internet at http://pubs.acs.org.

■ AUTHOR INFORMATION

Corresponding Author

*E-mail: gunnar.hansson@medkem.gu.se. Telephone: +46 31 7863488. Fax: +46 31 416108.

ABBREVIATIONS

Ag-PAGE, composite agarose-polyacrylamide gel electrophoresis; DOX, doxycycline; ER, endoplasmic reticulum; FBS, fetal bovine serum; IMDM, Iscove's modified Dulbecco's media; MUC2, mucin 2 (human); PC, principal component; PCA, principal component analysis; VWF, von Willebrand factor; WPB, Weibel−Palade bodies

REFERENCES

(1) Andersen, J. S.; Wilkinson, C. J.; Mayor, T.; Mortensen, P.; Nigg, E. A.; Mann, M. Proteomic characterization of the human centrosome by protein correlation profiling. *Nature* **2003**, *426*, 570−4.

(2) Dunkley, T. P.; Watson, R.; Griffin, J. L.; Dupree, P.; Lilley., K. S. Localization of organelle proteins by isotope tagging (LOPIT). *Mol. Cell. Proteomics* **2004**, *3*, 1128−34.

(3) Gilchrist, A.; Au, C. E.; Hiding, J.; Bell, A. W.; Fernandez-Rodriguez, J.; Lesimple, S.; Nagaya, H.; Roy, L.; Gosline, S. J.; Hallett, M.; Paiement, J.; Kearney, R. E.; Nilsson, T.; Bergeron, J. J. Quantitative proteomics analysis of the secretory pathway. *Cell* **2006**, *127*, 1265−81.

(4) Choi, H.; Fermin, D.; Nesvizhskii, A. I. Significance analysis of spectral count data in label-free shotgun proteomics. *Mol. Cell. Proteomics* **2008**, *7*, 2373−85.

(5) Foster, L. J.; de Hoog, C. L.; Zhang, Y.; Zhang, Y.; Xie, X.; Mootha, V. K.; Mann, M. A mammalian organelle map by protein correlation profiling. *Cell* **2006**, *125*, 187−99.

(6) Axelsson, M. A.; Asker, N.; Hansson, G. C. O-glycosylated MUC2 monomer and dimer from LS 174T cells are water-soluble, whereas larger MUC2 species formed early during biosynthesis are insoluble and contain nonreducible intermolecular bonds. *J. Biol. Chem.* **1998**, *273*, 18864−70.

(7) Godl, K.; Johansson, M. E.; Lidell, M. E.; Mörgelin, M.; Karlsson, H.; Olson, F. J.; Gum, J. R. Jr.; Kim, Y. S.; Hansson, G. C. The N terminus of the MUC2 mucin forms trimers that are held together within a trypsin-resistant core fragment. *J. Biol. Chem.* **2002**, *277*, 47248−56.

(8) Johansson, M. E.; Larsson, J. M.; Hansson, G. C. The two mucus layers of colon are organized by the MUC2 mucin, whereas the outer layer is a legislator of host-microbial interactions. *Proc. Natl. Acad. Sci. U.S.A.* **2011**, *108*, 4659−65.

(9) Johansson, M. E.; Phillipson, M.; Petersson, J.; Velcich, A.; Holm, L.; Hansson, G. C. The inner of the two Muc2 mucin-dependent mucus layers in colon is devoid of bacteria. *Proc. Natl. Acad. Sci. U.S.A.* **2008**, *105*, 15064−9.

(10) Van de Wetering, M.; Sancho, E.; Verweij, C.; de Lau, W.; Oving, I.; Hurlstone, A.; van der Horn, K.; Batlle, E.; Coudreuse, D.; Haramis, A. P.; Tjon-Pon-Fong, M.; Moerer, P.; van den Born, M.; Soete, G.; Pals, S.; Eilers, M.; Medema, R.; Clevers, H. The beta-catenin/TCF-4 complex imposes a crypt progenitor phenotype on colorectal cancer cells. *Cell* **2002**, *111*, 241−50.

(11) Laemmli, U. K. Cleavage of structural proteins during the assembly of the head of bacteriophage T4. *Nature* **1970**, *227*, 680−5.

(12) Schulz, B. L.; Packer, N. H.; Karlsson, N. G. Small-scale analysis of O-linked oligosaccharides from glycoproteins and mucins separated by gel electrophoresis. *Anal. Chem.* **2002**, *74*, 6088−97.

(13) Andersch-Björkman, Y.; Thomsson, K. A.; Holmén Larsson, J. M.; Ekerhovd, E.; Hansson, G. C. Large scale identification of proteins, mucins, and their O-glycosylation in the endocervical mucus during the menstrual cycle. *Mol. Cell. Proteomics* **2007**, *6*, 708−16.

(14) Cox, J.; Mann, M. MaxQuant enables high peptide identification rates, individualized p.p.b.-range mass accuracies and proteome-wide protein quantification. *Nat. Biotechnol.* **2008**, *26*, 1367−72.

(15) De Hoon, M. J.; Imoto, S.; Nolan, J.; Miyano, S. Open source clustering software. *Bioinformatics* **2004**, *20*, 1453−4.

(16) Hall, S. L.; Hester, S.; Griffin, J. L.; Lilley, K. S.; Jackson, A. P. The organelle proteome of the DT40 lymphocyte cell line. *Mol. Cell. Proteomics* **2009**, *8*, 1295−305.

(17) The UniProt Consortium. Ongoing and future developments at the Universal Protein Resource. *Nucleic Acids Res.* **2011**, *39*, D214−9.

(18) da Huang, W.; Sherman, B. T.; Lempicki, R. A. Systematic and integrative analysis of large gene lists using DAVID bioinformatics resources. *Nat. Protoc.* **2009**, *4*, 44−57.

(19) Tian, L.; Greenberg, S. A.; Kong, S. W.; Altschuler, J.; Kohane, I. S.; Park, P. J. Discovering statistically significant pathways in expression profiling studies. *Proc. Natl. Acad. Sci. U.S.A.* **2005**, *102*, 13544−9.

(20) Johansson, M. E.; Gustafsson, J. K.; Sjöber, K. E.; Petersson, J.; Holm, L.; Sjövall, H.; Hansson, G. C. Bacteria penetrate the inner mucus layer before inflammation in the dextran sulfate colitis model. *PLoS One* **2010**, *5*, e12238.

(21) Lodish, H. F.; Kong, N.; Hirani, S.; Rasmussen, J. A vesicular intermediate in the transport of hepatoma secretory proteins from the rough endoplasmic reticulum to the Golgi complex. *J. Cell Biol.* **1987**, *104*, 221−30.

(22) Johansson, M. E.; Thomsson, K. A.; Hansson, G. C. Proteomic analyses of the two mucus layers of the colon barrier reveal that their main component, the Muc2 mucin, is strongly bound to the Fcgbp protein. *J. Proteome Res.* **2009**, *8*, 3549−57.

(23) Takamatsu, H.; Takegahara, N.; Nakagawa, Y.; Tomura, M.; Taniguchi, M.; Friedel, R. H.; Rayburn, H.; Tessier-Lavigne, M.; Yoshida, Y.; Okuno, T.; Mizui, M.; Kang, S.; Nojima, S.; Tsujimura, T.; Nakatsuji, Y.; Katayama, I.; Toyofuku, T.; Kikutani, H.; Kumanogoh, A. Semaphorins guide the entry of dendritic cells into the lymphatics by activating myosin II. *Nat. Immunol.* **2010**, *11*, 594−600.

(24) Lam, P. P.; Hyvärinen, K.; Kauppi, M.; Cosen-Binker, L.; Laitinen, S.; Keränen, S.; Gaisano, H. Y.; Olkkonen, V. M. A cytosolic splice variant of Cab45 interacts with Munc18b and impacts on amylase secretion by pancreatic acini. *Mol. Biol. Cell* **2007**, *18*, 2473−80.

(25) Jerome-Majewska, L. A.; Achkar, T.; Luo, L.; Lupu, F.; Lacy, E. The trafficking protein Tmed2/p24beta(1) is required for morphogenesis of the mouse embryo and placenta. *Dev. Biol.* **2010**, *341*, 154−66.

(26) Logan, M. R.; Lacy, P.; Odemuyiwa, S. O.; Steward, M.; Davoine, F.; Kita, H.; Moqbel, R. A critical role for vesicle-associated membrane protein-7 in exocytosis from human eosinophils and neutrophils. *Allergy* **2006**, *61*, 777−84.

(27) Davis, C. W.; Dickey, B. F. Regulated airway goblet cell mucin secretion. *Annu. Rev. Physiol.* **2008**, *70*, 487−512.

(28) Valentijn, K. M.; van Driel, L. F.; Mourik, M. J.; Hendriks, G. J.; Arends, T. J.; Koster, A. J.; Valentijn, J. A. Multigranular exocytosis of Weibel-Palade bodies in vascular endothelial cells. *Blood* **2010**, *116*, 1807−16.

(29) Schonn, J. S.; van Weering, J. R.; Mohrmann, R.; Schlüter, O. M.; Südhof, T. C.; de Wit, H.; Verhage, M.; Sørensen, J. B. Rab3 proteins involved in vesicle biogenesis and priming in embryonic mouse chromaffin cells. *Traffic* **2010**, *11*, 1415–28.

(30) Coleman, W. L.; Bykhovskaia, M. Rab3a-mediated vesicle recruitment regulates short-term plasticity at the mouse diaphragm synapse. *Mol. Cell. Neurosci.* **2009**, *41*, 286–96.

(31) Wöllert, T.; Patel, A.; Lee, Y. L.; Provance, D. W. Jr.; Vought, V. E.; Cosgrove, M. S.; Mercer, J. A.; Langford, G. M. Myosin5a tail associates directly with Rab3A-containing compartments in neurons. *J. Biol. Chem.* **2011**, *286*, 14352–61.

(32) Specian, R. D.; Neutra, M. R. Mechanism of rapid mucus secretion in goblet cells stimulated by acetylcholine. *J. Cell Biol.* **1980**, *85*, 626–40.

(33) Min, S.-W.; Chang, W.-P.; Südhof, T. C. E-Syts, a family of membranous Ca2+-sensor proteins with multiple C2 domains. *Proc. Natl. Acad. Sci. U.S.A.* **2007**, *104*, 3823–8.

(34) Jean, S.; Mikryukov, A.; Tremblay, M. G.; Baril, J.; Guillou, F.; Bellenfant, S.; Moss, T. Extended-synaptotagmin-2 mediates FGF receptor endocytosis and ERK activation in vivo. *Dev. Cell* **2010**, *19*, 426–39.

(35) Kinouchi, K.; Ichihara, A.; Sano, M.; Sun-Wada, G. H.; Wada, Y.; Kurauchi-Mito, A.; Bokuda, K.; Narita, T.; Oshima, Y.; Sakoda, M.; Tamai, Y.; Sato, H.; Fukuda, K.; Itoh, H. The (pro)renin receptor/ ATP6AP2 is essential for vacuolar H+-ATPase assembly in murine cardiomyocytes. *Circ. Res.* **2010**, *107*, 30–4.

(36) Nelson, N. A journey from mammals to yeast with vacuolar H +-ATPase (V-ATPase). *J. Bioenerg. Biomembr.* **2003**, *35*, 281–9.

(37) Casey, J. R.; Grinstein, S.; Orlowski, J. Sensors and regulators of intracellular pH. *Nat. Rev. Mol. Cell. Biol.* **2010**, *11*, 50–61.

(38) Velcich, A.; Yang, W.; Heyer, J.; Fragale, A.; Nicholas, C.; Viani, S.; Kucherlapati, R.; Lipkin, M.; Yang, K.; Augenlicht, L. Colorectal cancer in mice genetically deficient in the mucin Muc2. *Science* **2002**, *295*, 1726–9.

(39) Andreyev, A. Y.; Shen, Z.; Guan, Z.; Ryan, A.; Fahy, E.; Subramaniam, S.; Raetz, C. R.; Briggs, S.; Dennis, E. A. Application of proteomic marker ensembles to subcellular organelle identification. *Mol. Cell. Proteomics* **2010**, *9*, 388–402.

(40) Neutra, M. R.; Phillips, T. L.; Phillips, T. E. Regulation of intestinal goblet cells in situ, in mucosal explants and in the isolated epithelium. *Ciba Found. Symp.* **1984**, *109*, 20–39.

(41) Specian, R. D.; Oliver, M. G. Functional biology of intestinal goblet cells. *Am. J. Physiol.* **1991**, *260*, C183–93.